J Therm Spray Tech (2018) 27:471–482
https://doi.org/10.1007/s11666-017-0677-8

PEER REVIEWED

Microstructure and Transparent Super-Hydrophobic Performance of Vacuum Cold-Sprayed Al_2O_3 and SiO_2 Aerogel Composite Coating

Jie Li[1] · Yu Zhang[1] · Kai Ma[1] · Xi-De Pan[1] · Cheng-Xin Li[1] · Guan-Jun Yang[1] · Chang-Jiu Li[1]

Submitted: 3 August 2017 / in revised form: 6 December 2017 / Published online: 16 January 2018

Abstract In this study, vacuum cold spraying was used as a simple and fast way to prepare transparent super-hydrophobic coatings. Submicrometer-sized Al_2O_3 powder modified by 1,1,2,2-tetrahydroperfluorodecyltriethoxysilane and mixed with hydrophobic SiO_2 aerogel was employed for the coating deposition. The deposition mechanisms of pure Al_2O_3 powder and Al_2O_3-SiO_2 mixed powder were examined, and the effects of powder structure on the hydrophobicity and light transmittance of the coatings were evaluated. The results showed that appropriate contents of SiO_2 aerogel in the mixed powder could provide sufficient cushioning to the deposition of submicrometer Al_2O_3 powder during spraying. The prepared composite coating surface showed rough structures with a large number of submicrometer convex deposited particles, characterized by being super-hydrophobic. Also, the transmittance of the obtained coating was higher than 80% in the range of visible light.

Keywords super-hydrophobicity · transparency · alumina · silica aerogel · vacuum cold spray

Introduction

Super-hydrophobic solid surfaces with water contact angle larger than 150° and sliding angle lower than 10° have received widespread attention over the years (Ref 1, 2). Initially, the super-hydrophobic phenomenon has been discovered through the natural surfaces, such as plant leaves (e.g., lotus leaves, rice leaves, and rose petals) and some parts of the animal bodies (e.g., butterfly wings and water strider's legs) (Ref 3, 4). These studies revealed that surface structure and surface free energy are the two factors determining the surface wettability, and surfaces with super-hydrophobic properties require low surface free energy and suitable rough structure morphologies (Ref 5, 6).

With the continuous development of industrial production, increasing attention has been paid to better understanding and studying of nature. Materials characterized by only one main functionality can hardly meet current requirements, so providing wide ranges of performances can broaden their applications. This initiated research on transparent super-hydrophobic surfaces, combining both super-hydrophobicity and transparency of surfaces. Super-hydrophobicity reduces the adhesion of water droplets on the surface; hence, the droplets can easily roll off and remove contaminant particles along the process, keeping the surface clean and dry (Ref 7). Therefore, transparent

✉ Xi-De Pan
xdpan@mail.xjtu.edu.cn

✉ Cheng-Xin Li
licx@mail.xjtu.edu.cn

Jie Li
crystallijie@163.com

Yu Zhang
1543356650@qq.com

Kai Ma
kaima_xjtu@foxmail.com

Guan-Jun Yang
ygj@mail.xjtu.edu.cn

Chang-Jiu Li
licj@mail.xjtu.edu.cn

[1] State Key Laboratory for Mechanical Behavior of Materials, School of Materials Science and Engineering, Xi'an Jiaotong University, Xi'an 710049, Shaanxi, People's Republic of China

super-hydrophobic surfaces have a wider range of potential applications. They may be used as self-cleaning glass, in building materials, electronic equipment screen, aircraft, cars, and spacecraft windshield glasses (Ref 8, 9).

To date, a large number of preparation methods of transparent super-hydrophobic surfaces have been developed, including *in situ* deposition (Ref 10), chemical vapor deposition (Ref 11), layer-by-layer assembly method (Ref 12), and etching (Ref 13). However, these methods suffer from numerous shortcomings, such as multiple step preparation, extreme conditions, and use of special instruments. In recent years, spray coating methods have been used for the preparation of transparent super-hydrophobic surfaces, including liquid flame spraying, spray pyrolysis technology, and suspension spraying. Using spray process, various materials (e.g., organic matter, oxides, and carbon nanotubes) can be deposited onto any substrate surface (e.g., glass, metal, and paper) (Ref 14-19). Due to their advantages in terms of simplicity, efficiency, and low-energy consumption, spray methods are considered promising for preparing transparent super-hydrophobic surfaces at large scale.

Vacuum cold spraying is one of the advanced simple and efficient spray technologies, mainly used for the preparation of ceramic coatings. The method is based on initial solid ceramic powder impacting the substrate at a certain speed to form coatings (Ref 20). Relevant reports showed that this method can deposit coatings with rough surface structures and good transparency. Hence, vacuum cold spraying is expected to yield transparent super-hydrophobic coatings (Ref 21, 22). Ceramics are widely used as functional materials, and thanks to their high hardness characteristic, it is possible to effectively improve the durability of the resulting coatings. Generally, the preparation of ceramic components requires high sintering temperatures. The joining of ceramic coatings with metals, glasses, and other materials with low melting points is usually difficult (Ref 23). Ceramic coatings produced by the conventional cold spraying method are often defective due to the poor deformation of brittle ceramic materials. Particles with high speeds will erode the substrate and the already deposited coatings (Ref 24). The emergence of vacuum cold spraying technology solves many of the above-mentioned limitations. The spraying conditions, including low absolute pressure, small starting particle size, and absence of gas preheating, induce particles with relatively low velocity and low temperature when impacting the substrate. This allows the particles to effectively deposit on the substrate. The technique has the ability to produce ceramic coatings with good performances without using high-temperature condition processing to coat almost any substrate (Ref 25). Moreover, many spray prepared coatings still have problems in terms of bond strength. Using vacuum cold spraying, a portion of the kinetic energy of the particles dissipated during collision with the substrate is converted to binding energy. Mechanical bonding can take place between the substrate-particle and particle-particle interfaces to form coatings with relatively high strength and adhesion, suitable for practical applications (Ref 23, 24).

In this study, vacuum cold spraying was used to deposit transparent super-hydrophobic coatings on glass substrates. Two common categories of materials used for preparing transparent components were selected as the deposited powders (Ref 9, 26). One of the powders was submicrometer Al_2O_3, the most widely used ceramic material. Because of its low price, the production cost will greatly reduce. Another powder material was loose porous SiO_2 aerogel added to Al_2O_3 powder during spraying to regulate the structures of the composite coating surfaces. This study aimed to discuss the deposition mechanisms of the powders with different structures, as well as the effects of powder on the structure, hydrophobicity, and transparency of the resulting coatings. The traditional method for preparing super-hydrophobic surface using hydrophilic materials aimed mainly to form surfaces with rough structures and then use low surface free energy materials to modify the surfaces (Ref 27). However, the modification reaction may not be sufficient and the modified layer could easily be damaged. The present research subverted the traditional preparation process, attempting to spray super-hydrophobic coatings directly by the materials with hydrophobic characteristics. Since Al_2O_3 has intrinsic hydrophilicity, first the powder was modified with fluorosilane to transfer to the hydrophobicity, while commercial SiO_2 aerogel powder had initial intrinsic hydrophobicity. The study discussed the feasibility of using hydrophobic materials to prepare super-hydrophobic surfaces with desirable low surface free energy. The proposed study may provide an innovative approach to prepare transparent super-hydrophobic surfaces through the vacuum cold spraying method.

Experimental

Materials

Two kinds of materials, Al_2O_3 (AL-160SG-3, Showa Denko, Japan) and SiO_2 aerogel (AEROSIL R106, Degussa, Germany), were used for spraying. The morphologies of the powders are shown in Fig. 1. The particle size of Al_2O_3 powder was in the submicrometer grade with size distribution of 200-500 nm. The particles showed angular morphologies and slight agglomeration (Fig. 1(a)). The commercially available SiO_2 aerogel was an intrinsic hydrophobic material. As shown in Fig. 1(b), the powder

was composed entirely of nanoparticles with an average size of 10 nm and exhibited soft agglomerated structure with micrometer sizes.

Commercially available glass slides (No. 7101, Sail Brand, China) with sizes of 75 × 25 × 1 mm were used as substrates. Before spraying, the substrates were cleaned with acetone and alcohol, respectively. Glass was selected because of its wide potential applications and high transparency to facilitate the detection of the transmittance of the coating.

The low surface energy material used in the experiment was 1,1,2,2-tetrahydroperfluorodecyltriethoxysilane (F-1060, SICONG, China), referred to as fluorosilane (FAS) with the chemical formula of $CF_3(CF_2)_7CH_2CH_2Si(OCH_2CH_3)_3$.

Powder Modification

Since Al_2O_3 had an intrinsic hydrophilicity, the powder was modified with fluorosilane to reduce its surface free energy. The procedure of the powder modification was performed as follows: 95 ml ethanol and 5 ml fluorosilane were first mixed to form a solution. The pH was adjusted to 11 using aqueous ammonia, and the mixture was ultrasonically stirred for 1 hour. Second, appropriate amount of Al_2O_3 powder (about 100 g) was mixed with 250 ml ethanol and stirred for 10 min to obtain a suspension. Next, the fluorosilane solution was added dropwise to the Al_2O_3 suspension and stirred for 18 h at room temperature using a magnetic stirrer, and the resulting powder was filtered off and then dried at 80 °C.

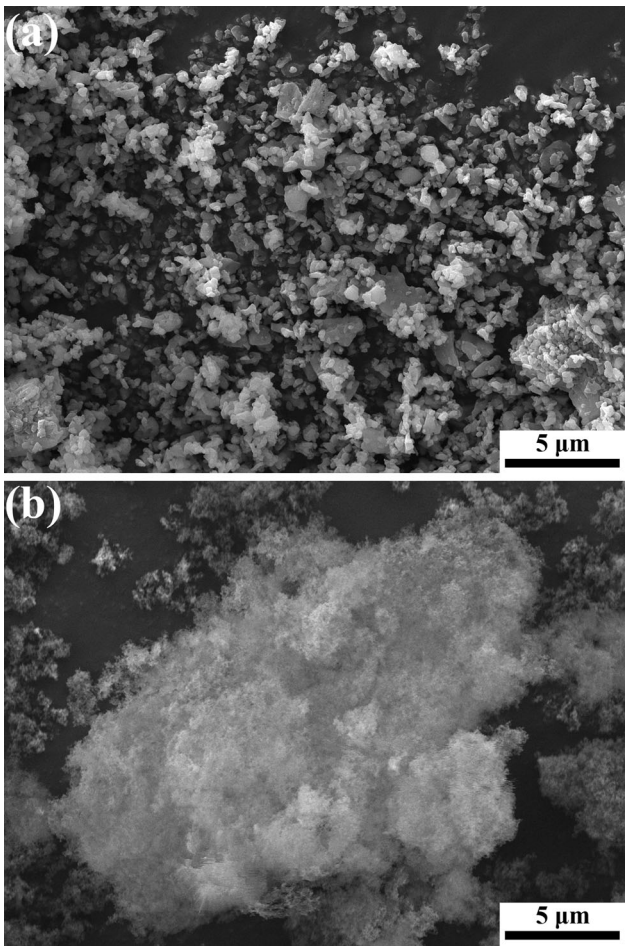

Fig. 1 Surface morphologies of the powders. (a) The submicrometer Al_2O_3 powder with particle sizes of 200-500 nm and (b) SiO_2 aerogel with soft agglomerates composed of large numbers of nanoparticles

Low-Energy Ball Milling

The previous literature showed that super-hydrophobic surfaces often had hierarchically rough structures (Ref 6). To yield suitable surface structures and study how the powder structure affect the coating structures and properties using vacuum cold spraying, hydrophobic SiO_2 aerogel was added to modified Al_2O_3 powder and mixed by low-energy ball milling. The parameters of low-energy ball milling are given in Table 1. Al_2O_3 powder and SiO_2 aerogel with four mass ratios were used for milling. The milling media was Al_2O_3 grinding ball with a diameter of 3 mm. Figure 2 shows typical morphology of the powder when Al_2O_3 particles were mixed with SiO_2 aerogel at the mass ratio of 3:1. The submicrometer particles were closely adhered by large numbers of nanoparticles. The mixed powder exhibited micrometer-sized cluster-like structures.

Coating Preparation

A home-developed vacuum cold spraying (VCS) system by Xi'an Jiaotong University was employed to deposit the modified Al_2O_3 and mixed powders (Fig. 3). During spraying, helium (He) was used as both the delivering powder and accelerating gas. The delivery powder gas entered the aerosolized feeder through the conduit. The particles were then effectively sent into the gun using the gas flow thanks to vibration of the feeder. With the accelerating gas, the particles would hit the substrate at certain speeds during deposition. The substrate was kept immobile, while the gun scanned in the X-Y plane and the powder sprayed evenly over the substrate surface.

Table 1 The low-energy ball milling parameters

Parameter	Value
Milling rotational speed (r min^{-1})	180
Ball milling time (h)	24
Mass ratio of ball to powder	10:1
Mass ratio of Al_2O_3 powder to SiO_2 aerogel	5:1/4:1/3:1/2:1

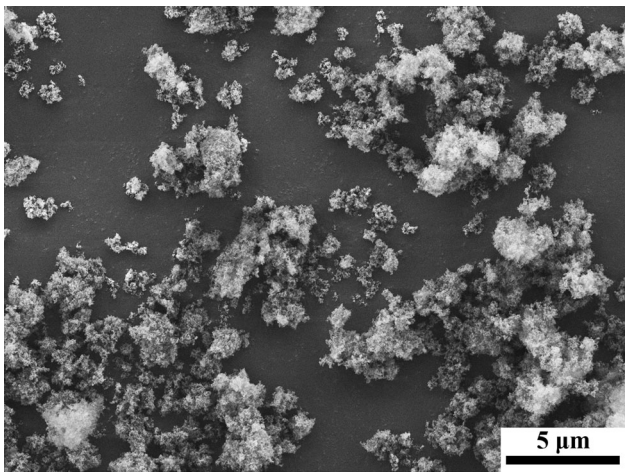

Fig. 2 Morphology of the mixed powder. The mass ratio of Al_2O_3 to SiO_2 is 3:1

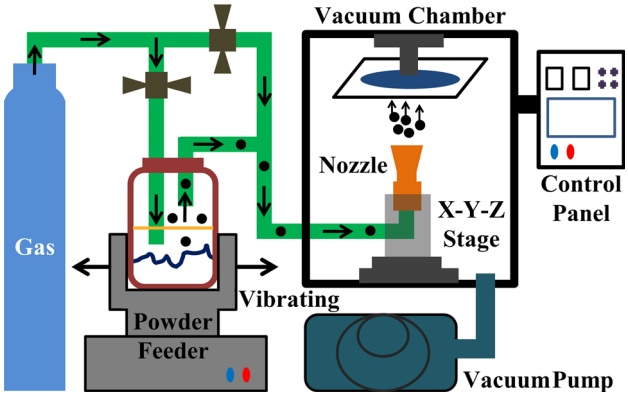

Fig. 3 Schematic diagram of the vacuum cold spraying system

Scanning the entire surface was considered as a 1 time spray process. In this study, rectangular copper with hollow size of 0.25 mm × 2.5 mm was used as the nozzle. Table 2 gathers the parameters used for vacuum cold spraying.

Characterization

Morphologies of feedstock powders and coatings were characterized by field emission scanning electron microscopy (MIRA3 LMH, TESCAN, Czech Republic). Surface roughness (Ra) was detected by laser scanning confocal microscopy (LSCM, VK9700K, Keyence, Japan). The static water contact angle (CA) and sliding angle (SA) measurements were carried out using a contact angle instrument (JC2000C4, Shanghai Zhongchen Digital Technic Apparatus Co., Ltd., China). The volume of the freshly deionized water droplet used for measurements was 5 µL. The static contact angle was measured using the sessile drop method by putting a water droplet on the horizontal coating surface followed by capturing an image and calculating the contact angle from the image. The sliding angle was measured by putting a water droplet on the horizontal coating surface followed by tilting the coating until the droplet started to move on the surface. The inclination angle of the coating was considered as the sliding angle. At least 5 droplets measurements were employed for each sample at different locations.

Table 2 Parameters of the vacuum cold spraying

Parameter	Unit	Value
Gas (He) flow rate	L min^{-1}	6
Chamber pressure	Pa	< 200
Gun traveling speed	mm s^{-1}	10
Spraying distance	mm	15
Times of spraying	Time	2

The chemical composition of the powder was detected by Fourier transform infrared spectroscopy (FTIR, Vertex70, Bruck, Germany) with a resolution of 4 cm^{-1} and 64 scans. The transmittance values of the coatings were collected with an ultraviolet-visible spectrophotometer (UV-3600, Shimadzu, Japan) in the range of 380-760 nm wavelengths. Soaking method and ultrasonic cleaning method were utilized for stability testing of the transparent super-hydrophobic coatings. The coating was first placed in alcohol at liquid depth of 6 mm, and using test time as a variable, the corresponding water contact angle and sliding angle on the surface were recorded after each test.

Results and Discussion

Characterization of Modified Al_2O_3 Powder

The infrared spectra of Al_2O_3 powders before and after modification by fluorosilane are shown in Fig. 4. The chemical groups associated with hydroxyl and oxide were detected on the original powder surface, where the transmission peak around 3432 cm^{-1} was assigned to the stretching vibration of O-H and that at 627 cm^{-1} represented the oxide (Ref 28). Since the surface free energies of hydroxyl and metal oxide are greater than that of water, the original powder exhibited hydrophilicity (Ref 29). It can be observed that the water droplets can rapidly penetrate into the tablet surface after the original powder was tabletted (inset image in Fig. 4(a)).

For the modified powder, water droplets remained standing on the surface and exhibited spherical shapes after the powder was tabletted (inset image in Fig. 4(b)), indicating that the powder was hydrophobic. The FTIR data

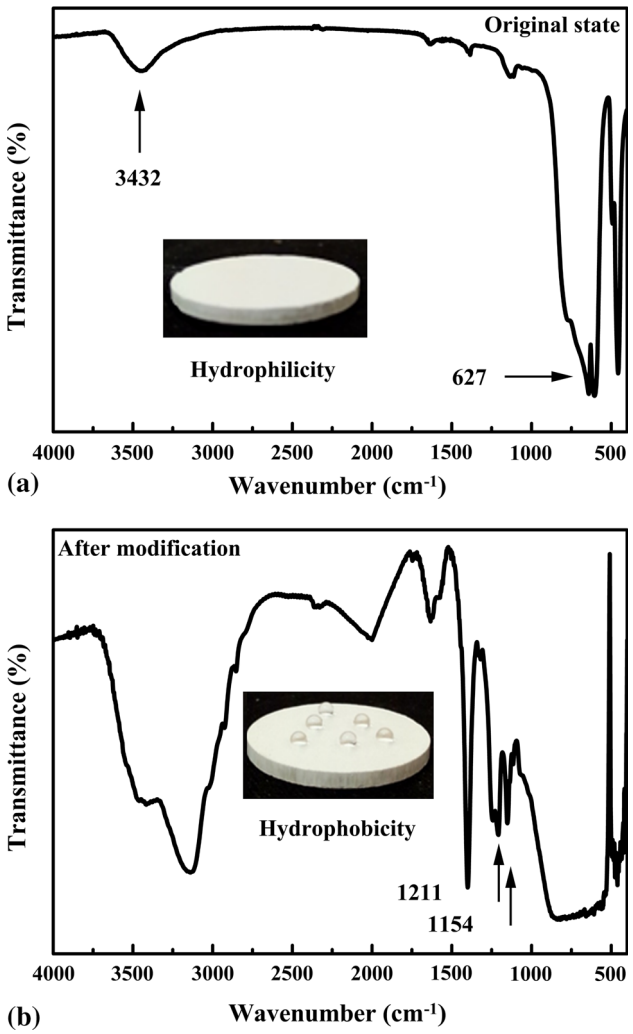

Fig. 4 Comparison of infrared spectra of the powders. (a) Original powder and (b) modified powder. Inserted images show the droplets states on the powders tablet surfaces

showed that the asymmetric stretching vibration and symmetrical stretching vibration of -CF_2 were located at 1211 and 1154 cm^{-1}, further confirming that the particle surface was grafted with fluorosilane molecules with low surface free energy (Ref 30). The mechanism of powder modification process is presented in Fig. 5. First, the fluorosilane was hydrolyzed by replacing the three ethoxy groups attached to the Si atom by the hydroxyl groups. Afterward, the hydroxyl groups present on both the fluorosilane and particle surface underwent dehydration condensation, where low surface energy fluorocarbon chains were grafted onto the particle surface (Ref 31). Meanwhile, dehydration reaction occurred between the hydrolyzed fluorosilane molecules, forming a network of fluorosilane molecular chain on the surface. During this process, the powder particle surface was expected to sufficiently be covered by low surface free energy molecules. In addition, it will be noted that the modification process did not change the morphology of the original Al_2O_3 powder as revealed by SEM. In other words, the morphology of the modified powder was basically the same as that of the powder shown in Fig. 1(a).

Coating Deposition Using Modified Al_2O_3 Powder

First, the modified Al_2O_3 powder was used to deposit coatings on glass substrates by vacuum cold spraying. Figure 6 shows the morphology of the coating surface under different magnifications. The particles were uniformly deposited on the substrate surface in a flattened manner to form a flat surface. The average roughness (Ra) of the surface detected by LSCM was 0.195 ± 0.008 μm.

Figure 7 depicts the light transmittance of the glass substrate and deposited coating. It can be seen that the transmittance in the visible range of Al_2O_3 coating reached a value about 95%, almost the same as the glass substrate. The deposited coating illustrated good light transmittance. Some studies found that Al_2O_3 is an intrinsic transparent material since both its grain boundary reflection and scattering losses could be ignored. Therefore, Al_2O_3 was commonly used in the preparation of transparent components (Ref 32, 33). The good light transmittance of the coating indicated small surface roughness and high density of the coating, which greatly inhibited light scattering.

The evaluation of surface wettability revealed the smooth glass substrate surface to be hydrophilic with water contact angle of only 23.6° ± 3.2°. When Al_2O_3 coating was deposited on the substrate, the water contact angle value increased to 107.1° ± 1.7°. An image of the water droplet on the surface is shown in Fig. 6(a). The deposited Al_2O_3 coating surface showed hydrophobicity, indicating that the surface chemical state of the powder did not change and its hydrophobic characteristic was retained during spraying. On the other hand, the hydrophobic coating surface can be obtained by direct deposition of the modified powder. However, since water droplets cannot roll on the surface and pinned to it, the surface failed to gain super-hydrophobicity. This was presumably caused by the flat surface structure and low surface roughness. Therefore, appropriate surface roughness was necessary for excellent hydrophobicity of the coating surface.

Coatings Deposition Using Mixed Powders

SiO_2 is a low light-absorbing material commonly used for preparing transparent components, similar to Al_2O_3 (Ref 17, 34). To induce relevant structures in terms of super-hydrophobicity and transparency of the coating, hydrophobic SiO_2 aerogel with various proportions was added to the modified Al_2O_3 powder to deposit the coating.

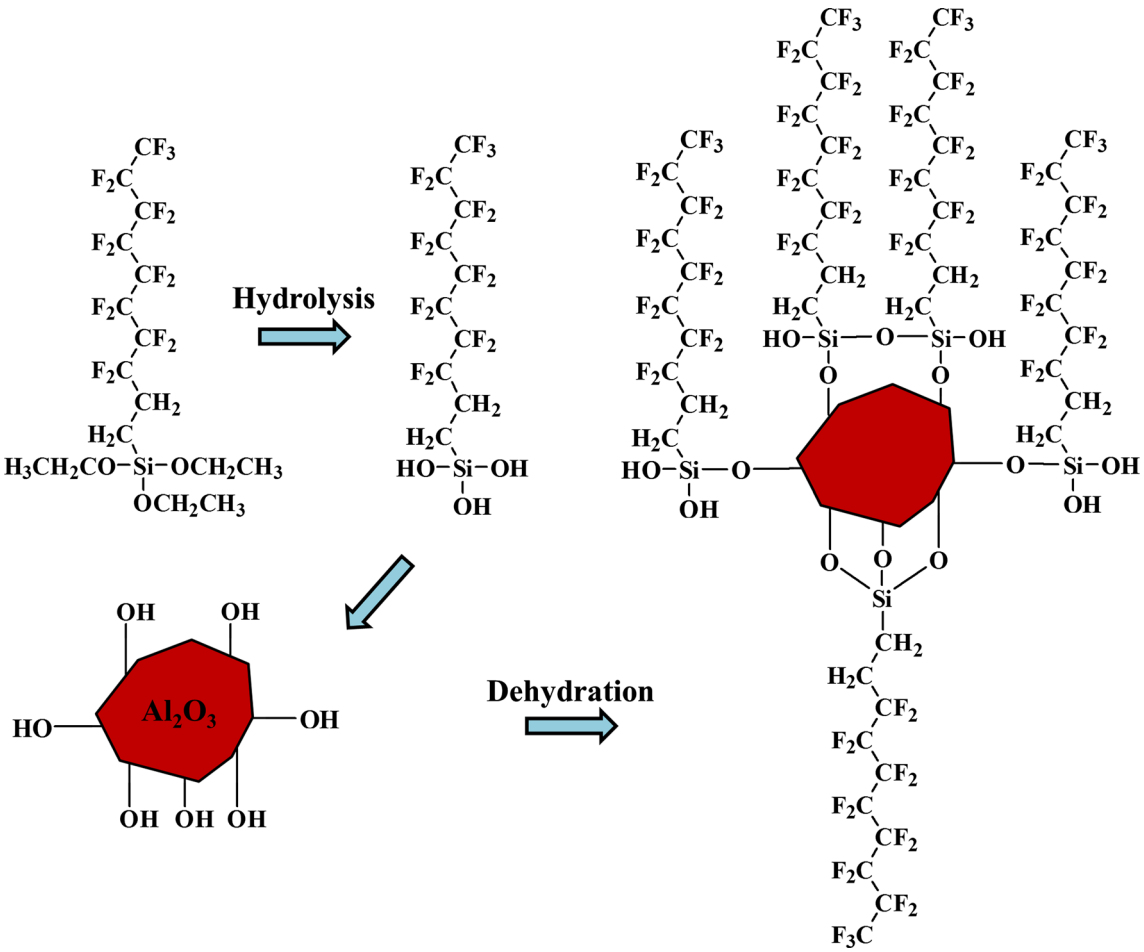

Fig. 5 Schematic representation of the powder modification process

The effect of powder structure on the coating structure and its properties were then evaluated. Four sets of mixed Al_2O_3 powder and SiO_2 aerogel with different mass ratios are listed in Table 1 and were prepared by low-energy ball milling.

Compared to the coating surface deposited by single Al_2O_3 powder, the surface wettability showed improvements in surface hydrophobicity when SiO_2 aerogel was added to Al_2O_3 powder (Fig. 8). As the proportion of SiO_2 aerogel increased in the mixed powder, the coating surface exhibited different hydrophobicities. At mass ratios of Al_2O_3 powder and SiO_2 aerogel of 5:1 and 4:1, the contact angle of water droplets on coating surfaces raised to 129.2° ± 1.7° and 135.5° ± 1.5°, respectively. Unfortunately, water droplets still pinned on the surfaces and cannot roll freely, showing hydrophobic surfaces. When the mass ratio reached 3:1, the contact angle of the droplet on the surface rose to 153.8° ± 0.9°. In addition, the droplet can quickly roll off from the surface when the coating was tilted by 2°. In this case, the prepared coating surface was super-hydrophobic. The continuous increase in SiO_2 aerogel content in the mixed powder to reach a mass ratio of 2:1 reduced the water contact angle to 145.5° ± 1.2° and raised the sliding angle to 16.0° ± 0.5°.

The addition of SiO_2 aerogel into the Al_2O_3 powder also affected the light transmittance of the coatings. Figure 9 shows the light transmission of the composite coatings. As the content of SiO_2 aerogel in the mixed powder increased, the light transmittance of the coating gradually decreased. The coatings prepared by mixed powders with mass ratios of Al_2O_3 powder to SiO_2 aerogel of 5:1 and 4:1 showed excellent transparencies with light transmittance near 90% in the range of visible light. At mass ratio of 3:1, the light transmission of the coating decreased, but the coating was still transparent with light transmittance above 80%. However, the light transmittance of the coating deposited by powder at mixing ratio of 2:1 was only 70%-80%, showing translucent properties. Overall, the above data revealed that the coating prepared by mixed powder at ratio of 3:1 was super-hydrophobic with good light transmittance.

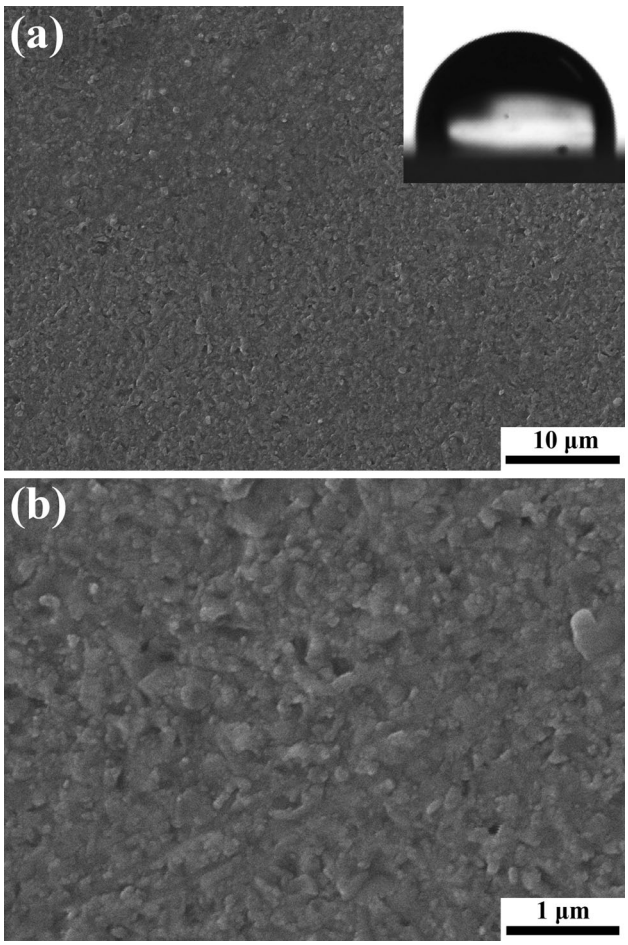

Fig. 6 Morphology of the coating surface deposited by modified Al_2O_3 powder under different magnifications. The inset image shows the water droplet standing on the coating surface with static contact angle of 107.1°

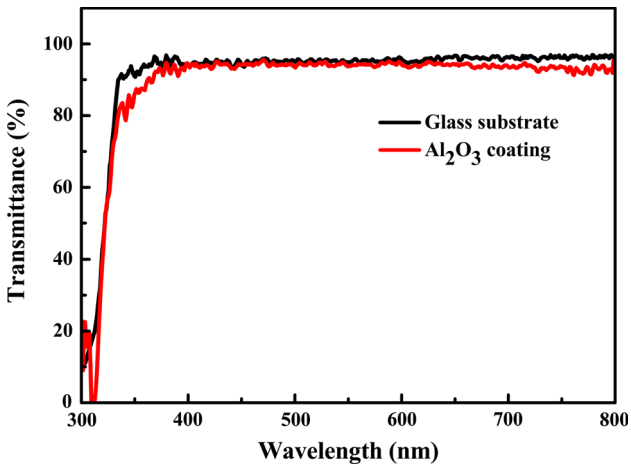

Fig. 7 The transmittance of the glass substrate and Al_2O_3 coating

The coating structure often influences surface wettability and transmittance of the coating. The SEM images of the coating prepared by mixed powders are shown in Fig. 10, and surface roughness values of the resulting coatings measured by LSCM are listed in Table 3. As the proportion of SiO_2 aerogel in the mixed powder increased, both the surface structure and surface roughness obviously changed. At the mass ratio of Al_2O_3 powder to SiO_2 aerogel of 5:1 and 4:1, the coating surface remained relatively flat (Fig. 10(a, b)). However, the surface roughness of the coatings improved as compared to the surface deposited by single Al_2O_3 powder. The above-mentioned coating surfaces were hydrophobic, but water droplets cannot roll on the surface, indicating that the rough surface structure preventing movement of the droplets, the liquid may fill in the depression area of the rough structure. The contact of the droplets with the surface can be regarded as in the Wenzel state, predicting that the contact angles of droplets on hydrophobic surfaces increased as surface roughness rose (Ref 35). Therefore, the increase in roughness led to improvements in surface hydrophobicity.

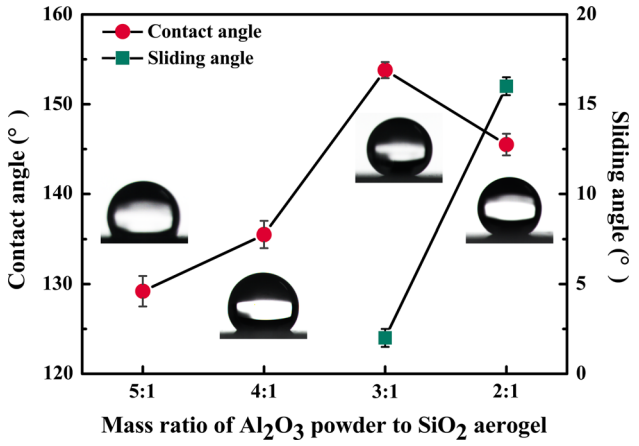

Fig. 8 Water contact angle and sliding angle of the coating surface deposited by Al_2O_3 powder and SiO_2 aerogel mixed at different mass ratios

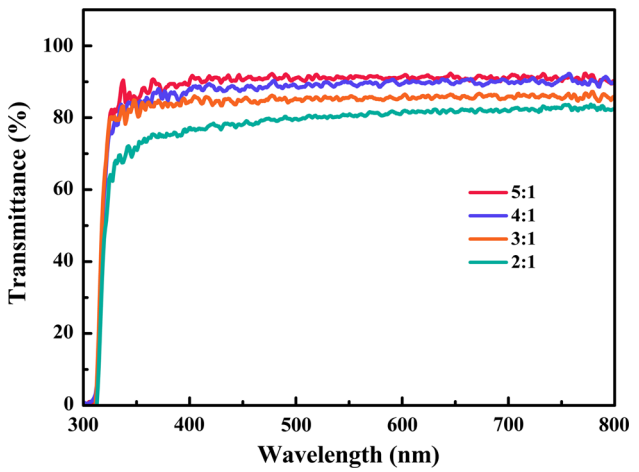

Fig. 9 The transmittance of the composite coatings deposited by Al_2O_3 powder and SiO_2 aerogel mixed at different mass ratios

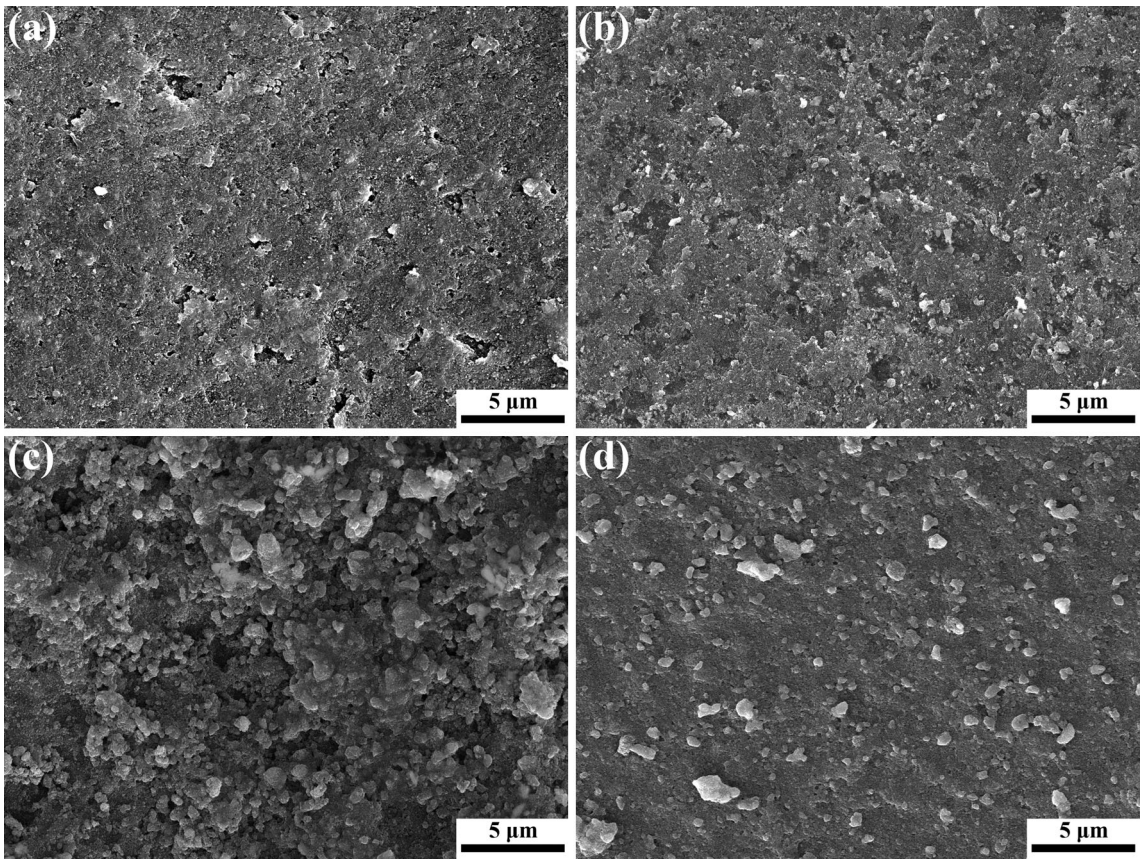

Fig. 10 The coating surface deposited by Al_2O_3 powder and SiO_2 aerogel mixed at different mass ratios. The mass ratios of Al_2O_3 powder to SiO_2 aerogel are: (a) 5:1, (b) 4:1, (c) 3:1, and (d) 2:1

Table 3 Surface roughness of the coatings

Mass ratio of Al_2O_3 to SiO_2	Ra, μm
5:1	0.217 ± 0.005
4:1	0.224 ± 0.009
3:1	0.294 ± 0.005
2:1	0.275 ± 0.003

Thus, the contact angle of the surface deposited by mixed powder was superior to that prepared by single Al_2O_3. At the mass ratio of 3:1, large numbers of submicrometer-sized particles were deposited on the surface (Fig. 10(c)), and the surface roughness of the coating reached a maximum value of 0.294 ± 0.005 μm. Since the coating contained undulating rough structure formed by large numbers of submicrometer particles, the recessed area formed by the rough structure can form large numbers of air cushions, which could effectively prevent the droplets from penetrating into the rough structure. In this case, the droplets were in the Cassie-Baxter state on the surface (Ref 35). This state reduced the contact area between the droplet and the surface, which greatly increased the contact angle of the droplet and decreased the resistance of the surface to droplet movement. This yielded super-hydrophobic surfaces. However, at the ratio of 2:1, the coverage density of the submicrometer particles on the coating surface obviously decreased, as shown in Fig. 10(d). The surface roughness of the coating slightly decreased, resulting in reduced hydrophobicity.

The factors affecting the transparency of coatings are mainly the surface roughness and density, implying the introduction of sources of light scattering. Nakajima et al. (Ref 36) suggested that to maintain the transparency of materials in the visible wavelength range (380-760 nm), surface roughness should be either lower or much higher than the range. Table 3 indicates that surface roughness (Ra) values of the four different surfaces were all lower than the visible wavelength. Therefore, surface roughness of the coating was small enough to inhibit light scattering. The internal structure of the coating may be the main factor affecting the light transmittance of the prepared coatings. The light transmission results of the coatings suggested that addition of SiO_2 aerogel during deposition decreased the density of the coating, which should be the reason for the declined light transmittance of the coating (Ref 37, 38).

Deposition Mechanism of Particles

The results mentioned above showed that the coating structure significantly affects their properties. By spraying either single Al_2O_3 powder or mixed powders, the coating structure can effectively be controlled by adjusting the powder structure by vacuum cold spraying.

For Al_2O_3 powder, the coating surface was composed of large numbers of flattened particles shown in Fig. 6. The cross-sectional morphology of the coating is depicted in Fig. 11(a). The cohesion of the particles appeared good, and the coating was very dense. The average size of the particles in the coating is smaller than that of the original submicrometer particles. The particles were also well flattened, indicating that they underwent fracture and plastic deformation at high impact velocities during spraying. These data were consistent with related published reports (Ref 25, 39). The deposition mechanism of the powder is summarized in Fig. 12(a). During particles collision with the substrate at high speed, a great force was produced, resulting in fracture and deformation of the particles. Coupled with the hammering effect produced by subsequent bombarding particles in the deposition process, a coating with relatively flat surface morphology and dense internal structure was generated (Ref 23). Such coating structure induced excellent light transmission but poor surface hydrophobicity.

The average particle size of SiO_2 aerogel was estimated to be in the nanometer scale with loose agglomerated particles (Fig. 1(b)). The density of aerogel was small, where more than 90% of powder composition was air. Therefore, large amounts of space as void existed inside the aerogel. When SiO_2 aerogel was added to the submicrometer Al_2O_3 powder for coating deposition at mass ratio of Al_2O_3 powder to SiO_2 aerogel of 3:1, the coating surface became rough and large numbers of submicrometer particles formed when compared to single alumina-deposited coating surface. Figure 11 (b) illustrates the cross-sectional morphology of the coating. The addition of SiO_2 aerogel during deposition reduced the degree of fragmentation of Al_2O_3 particles, inducing large amounts of bigger particles inside the coating. The morphology of mixed powder in Fig. 2 showed larger particles intimately adhered by large numbers of nano aerogel particles, forming mixed powder with micrometer-sized cluster-like structures. During the deposition process, presence of large numbers of voids in the aerogel may provide a buffering effect for deposition of submicrometer particles, thereby reducing the

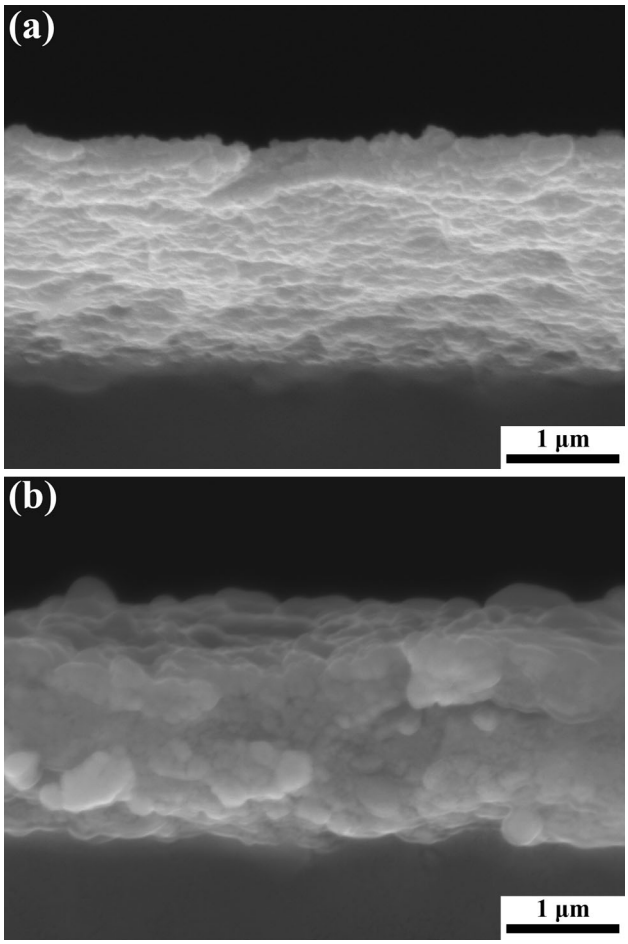

Fig. 11 Cross-sectional morphologies of the coatings. (a) Single submicrometer Al_2O_3 powder and (b) mixed powder of submicrometer Al_2O_3 and SiO_2 aerogel at the mass ratio of 3:1

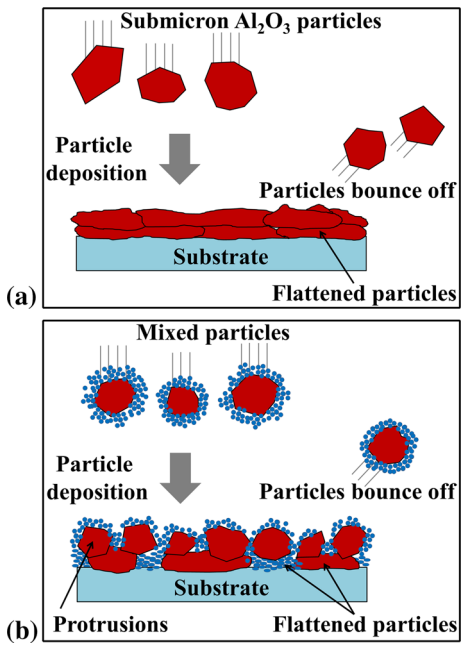

Fig. 12 The deposition mechanism of the powders with different structures during vacuum cold spraying. (a) Single submicrometer Al_2O_3 powder and (b) mixed powder of submicrometer Al_2O_3 and SiO_2 aerogel

fragmentation and flattening degree of the submicrometer particles. This, in turn, resulted in large numbers of bigger particles on the coating surface and inside it. The deposition mechanism is summarized in Fig. 12(b). The rough surface structure was conducive to reducing the solid-liquid contact area and promoting the surface super-hydrophobicity. However, the buffering effect of the aerogel may reduce the hammering effect of the submicrometer Al_2O_3 particles on the coating, resulting in decreased density of the internal structure of the coating. This result subsequently increased light scattering of the coating and declined the transparency.

The content of silica aerogels in the mixed powder would also affect the coating structure. At smaller contents of aerogel in the mixed powder (mass ratios of Al_2O_3 to SiO_2 of 5:1 and 4:1), the added amount of the aerogel was too small to significantly alter the deposition behavior of the Al_2O_3 particles. Therefore, the structure and properties of the coating did not significantly change when compared to that of single Al_2O_3-deposited coating. With the mixed powder with larger contents of aerogel (mass ratios of Al_2O_3 to SiO_2 of 2:1), the deposition was mainly based on SiO_2 particles and only small amounts of submicrometer Al_2O_3 particles were deposited on the surface (Fig. 10(d)). Thus, it can be speculated that the decrease in submicrometer particle content would weaken the hammering effect of the particles on the coating, decreasing the coating density, and affecting its light transmission performance. As a result, the suitable coating structures with good performances would require particles with matched sizes.

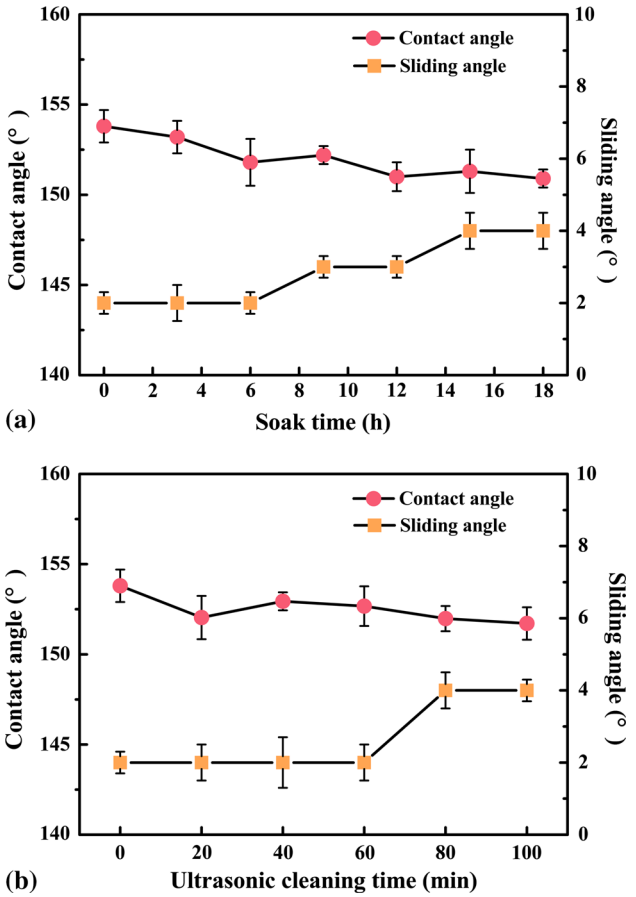

Fig. 13 The variation of water contact angle and sliding angle of the super-hydrophobic surface as a function of testing time. (a) Soaking in alcohol and (b) ultrasonic cleaning with alcohol

Stability of Super-Hydrophobic Coating Surface

The stability of super-hydrophobic coating surface highly affects the practical applications. To evaluate the stability, the transparent super-hydrophobic coatings prepared with mixed powders at a mass ratio of Al_2O_3 to SiO_2 of 3:1 were subjected to alcohol soaking and alcohol ultrasonic cleaning treatment, respectively. The changes in contact angle and sliding angle of the coatings are shown in Fig. 13. After soaking in alcohol or ultrasonic cleaning with alcohol for some time, the wettability of the super-hydrophobic surface slightly varied. The water contact angle on the surface is still greater than 150°, and sliding angle is lower than 10°. Meanwhile, the transparency of the coating remained unchanged during the treatment. The above results indicated that the combination of the fluorosilane assembled on the coatings and the bonding of the coatings were strong enough to yield films with relevant properties. The prepared transparent super-hydrophobic surface showed certain stability. However, the adhesion strength and abrasion resistance are two important criteria for evaluating the feasibility of coatings in practical use; thus, relevant performance still requires further investigation.

Conclusions

Vacuum cold spraying method was used to prepare transparent super-hydrophobic coatings. The results showed that deposited fluorosilane-modified submicrometer Al_2O_3 surface was relatively flat and the coating was dense. The surface hydrophobicity was poor, but light transmittance was excellent. The addition of appropriate amounts of loose SiO_2 aerogel to the submicrometer Al_2O_3 powder during the deposition formed suitable coating structure meeting the performance requirements thanks to the aerogel which provided sufficient cushioning for the Al_2O_3 deposition. At the mass ratio of Al_2O_3 powder to SiO_2 aerogel of 3:1, the coating surface presented rough structure with large numbers of submicrometer convex deposited particles, satisfying the conditions of super-hydrophobicity. However, the coating structure did not

cause severe light scattering, and light transmission of the coating was more than 80% in the range of visible light. When subjected to immersion or ultrasonic cleaning with alcohol, the coatings still maintained super-hydrophobicity and good light transmission. The proposed vacuum cold spraying method with simple operation and high efficiency would be promising to extend the potential applications of transparent super-hydrophobic coatings to waterproof glass, protective films, and electronic equipment screens, among others.

Acknowledgments This work was supported by the National Basic Research Program of China [2012CB625100].

References

1. X. Zhang, F. Shi, J. Niu, Y. Jiang, and Z. Wang, Superhydrophobic Surfaces: From Structural Control to Functional Application, *J. Mater. Chem.*, 2008, **18**(6), p 621-633
2. H. Ogihara, J. Xie, and T. Saji, Factors Determining Wettability of Superhydrophobic Paper Prepared by Spraying Nanoparticle Suspensions, *Colloid. Surface A*, 2013, **434**(19), p 35-41
3. W. Barthlott and C. Neinhuis, Purity of the Sacred Lotus, or Escape from Contamination in Biological Surfaces, *Planta*, 1997, **202**(1), p 1-8
4. C. Neinhuis and W. Barthlott, Characterization and Distribution of Water-repellent, Self-Cleaning Plant Surfaces, *Ann. Bot.*, 1997, **79**(6), p 667-677
5. J.M. Lim, G.R. Yi, J.H. Moon, C.J. Heo, and S.M. Yang, Superhydrophobic Films of Electrospun Fibers with Multiple-Scale Surface Morphology, *Langmuir*, 2007, **23**(15), p 7981-7989
6. L. Feng, S. Li, Y. Li, H. Li, L. Zhang, Y. Song, B. Liu, L. Jiang, and D. Zhu, Super-Hydrophobic Surfaces: From Natural to Artificial, *Adv. Mater.*, 2002, **14**(24), p 1857-1860
7. R. Fürstner and W. Barthlott, Wetting and Self-Cleaning Properties of Artificial Superhydrophobic Surfaces, *Langmuir*, 2005, **21**(3), p 956-961
8. J.H. Kong, T.H. Kim, J.H. Kim, J.K. Park, D.W. Lee, S.H. Kim, and J.M. Kim, Highly Flexible, *Transparent and Self-Cleanable Superhydrophobic Films Prepared by a Facile and Scalable Nanopyramid Formation Technique, Nanoscale*, 2014, **6**(3), p 1453-1461
9. S.G. Lee, D.S. Ham, D.Y. Lee, H. Bong, and K. Cho, Transparent Superhydrophobic/Translucent Superamphiphobic Coatings Based on Silica-Fluoropolymer Hybrid Nanoparticles, *Langmuir*, 2013, **29**(48), p 15051-15057
10. G. Wang, W. Liang, B. Wang, Y. Zhang, J. Li, L. Shi, and Z. Guo, Conductive and Transparent Superhydrophobic Films on Various Substrates by In Situ Deposition, *Appl. Phys. Lett.*, 2013, **102**(20), p 203703
11. K. Teshima, H. Sugimura, Y. Inoue, O. Takai, and A. Takano, Transparent Ultra Water-Repellent Poly(Ethylene Terephthalate Substrates Fabricated by Oxygen Plasma Treatment and Subsequent Hydrophobic Coating, *Appl. Surf. Sci.*, 2005, **244**(1-4), p 619-622
12. J. Bravo, L. Zhai, Z. Wu, R.E. Cohen, and M.F. Rubner, Transparent Superhydrophobic Films Based on Silica Nanoparticles, *Langmuir*, 2007, **23**(13), p 7293-7298
13. A. Nakajima, K. Abe, K. Hashimoto, and T. Watanabe, Preparation of Hard Super-Hydrophobic Films with Visible Light Transmission, *Thin Solid Films*, 2000, **376**(1), p 140-143
14. H. Teisala, M. Tuomine, M. Aromaa, J.M. Mäkelä, M. Stepien, J.J. Saarinen, M. Toivakka, and J. Kuusipalo, Development of Superhydrophobic Coating on Paperboard Surface Using the Liquid Flame Spray, *Surf. Coat. Tech.*, 2010, **205**(2), p 436-445
15. N.L. Tarwal and P.S. Patil, Superhydrophobic and Transparent ZnO Thin Films Synthesized by Spray Pyrolysis Technique, *Appl. Surf. Sci.*, 2010, **256**(24), p 7451-7456
16. J. Yang, Z. Zhang, X. Men, and X. Xu, Fabrication of Stable, Transparent and Superhydrophobic Nanocomposite Films with Polystyrene Functionalized Carbon Nanotubes, *Appl. Surf. Sci.*, 2009, **255**(22), p 9244-9247
17. P. Wang, J. Liu, W. Chang, X. Fan, C. Li, and Y. Shi, A Facile Cost-Effective Method for Preparing Robust Self-Cleaning Transparent Superhydrophobic Coating, *Appl. Phys. A-Mater.*, 2016, **122**(10), p 916
18. W. Yao, K.J. Bae, M.Y. Jung, and Y.R. Cho, Transparent, Conductive, and Superhydrophobic Nanocomposite Coatings on Polymer Substrate, *J. Colloid Interface Sci.*, 2017, **506**, p 429-436
19. H.S. Hwang, N.H. Kim, S.G. Lee, D.Y. Lee, K. Cho, and I. Park, Facile Fabrication of Transparent Superhydrophobic Surfaces by Spray Deposition, *ACS Appl. Mater. Inter.*, 2011, **3**(7), p 2179-2183
20. S.Q. Fan, C.J. Li, C.X. Li, G.J. Liu, G.J. Yang, and L.Z. Zhang, Preliminary Study of Performance of Dye-Sensitized Solar Cell of Nano-TiO_2 Coating Deposited by Vacuum Cold Spraying, *Mater. Trans.*, 2006, **47**(7), p 1703-1709
21. Y. Sato, Y. Uemichi, K. Nishikawa, and S. Yoshikado, Fabrication of Al_2O_3 Films Using Aerosol Deposition Method and Their Characterization, *IOP Conf. Ser.: Mater. Sci. Eng.*, 2011, **18**, p 092056
22. J. Akedo, Aerosol Deposition Method for Fabrication of Nano Crystal Ceramic Layer, *Mater. Sci. Forum*, 2004, **43-48**, p 449-452
23. D. Hanft, J. Exner, M. Schubert, T. Stöcker, P. Fuierer, and R. Moos, An Overview of the Aerosol Deposition Method: Process Fundamentals and New Trends in Materials Applications, *J. Ceram. Sci. Technol.*, 2015, **6**(3), p 147-182
24. J.O. Kliemann, H. Gutzmann, F. Gärtner, H. Hübner, C. Borchers, and T. Klassen, Formation of Cold-Sprayed Ceramic Titanium Dioxide Layers on Metal Surfaces, *J. Therm. Spray Technol.*, 2011, **20**(1-2), p 292-298
25. J. Akedo, Room Temperature Impact Consolidation (RTIC) of Fine Ceramic Powder by Aerosol Deposition Method and Applications to Microdevices, *J. Therm. Spray Technol.*, 2008, **17**(2), p 181-198
26. T. Aytug, J.T. Simpson, A.R. Lupini, R.M. Trejo, G.E. Jellison, I.N. Ivanov, S.J. Pennycook, D.A. Hillesheim, K.O. Winter, D.K. Christen, S.R. Hunter, and J.A. Haynes, Optically Transparent, Mechanically Durable, Nanostructured Superhydrophobic Surfaces Enabled by Spinodally Phase-Separated Glass Thin Films, *Nanotechnology*, 2013, **24**(31), p 315602
27. J. Drelich, E. Chibowski, D.D. Meng, and K. Terpilowski, Hydrophilic and Superhydrophilic Surfaces and Materials, *Soft Matter*, 2011, **7**(21), p 9804-9828
28. G. Verma, S.K. Dhoke, and A.S. Khanna, Polyester Based-Siloxane Modified Waterborne Anticorrosive Hydrophobic Coating on Copper, *Surf. Coat. Technol.*, 2012, **212**(6), p 101-108
29. S. Takeda, M. Fukawa, Y. Hayashi, and K. Matsumoto, Surface OH Group Governing Adsorption Properties of Metal Oxide Films, *Thin Solid Films*, 1999, **339**(1-2), p 220-224
30. W. Xu, J. Song, J. Sun, Y. Lu, and Z. Yu, Rapid Fabrication of Large-Area, Corrosion-Resistant Superhydrophobic Mg Alloy Surfaces, *ACS Appl. Mater. Inter.*, 2011, **3**(11), p 4404-4414
31. S.R. Yu, J.A. Liu, W. Diao, and W. Li, Preparation of a Bionic Microtexture on X52 Pipeline Steels and Its Superhydrophobic Behavior, *J. Alloys Compd.*, 2014, **585**(5), p 689-695

32. H. Yoon, H. Kim, S.S. Latthe, M.W. Kim, S. Al-Deyab, and S.S. Yoon, A Highly Transparent Self-Cleaning Superhydrophobic Surface by Organosilane-Coated Alumina Particles Deposited via Electrospraying, *J. Mater. Chem. A*, 2015, **3**(21), p 11403-11410
33. B.E. Yoldas, A Transparent Porous Alumina, *Am. Ceram. Soc. Bull.*, 1975, **54**(3), p 286-288
34. X. Meng, Y. Wang, H. Wang, J. Zhong, and R. Chen, Preparation of the Multifunctional Antireflective Films from a Templating Composite Silica Sol with Entwining Structures, *Surf. Coat. Technol.*, 2013, **236**(2), p 518-524
35. B. Bhushan and Y.C. Jung, Natural and Biomimetic Artificial Surfaces for Superhydrophobicity, Self-Cleaning, Low Adhesion, and Drag Reduction, *Mater. Sci.*, 2011, **56**(1), p 1-108
36. A. Nakajima, Design of a Transparent Hydrophobic Coating, *J. Ceram. Soc. Jpn.*, 2004, **112**(1310), p 533-540
37. M. Nakada, H. Tsuda, K. Ohashi, and J. Akedo, Aerosol Deposition on Transparent Electro-Optic Films for Optical Modulators, *IEICE T. Electron.*, 2007, **E90-C**(1), p 36-40
38. R. Apetz and M.P.B. van Bruggen, Transparent Alumina: A Light-Scattering Model, *J. Am. Ceram. Soc.*, 2010, **86**(3), p 480-486
39. J. Akedo, Aerosol Deposition of Ceramic Thick Films at Room Temperature: Densification Mechanism of Ceramic Layers, *J. Am. Ceram. Soc.*, 2006, **89**(6), p 1834-1839